Chin. J. Chem. Eng., **15**(3) 339—344 (2007)

Voidage Measurement of Gas-Oil Two-phase Flow*

WANG Weiwei(王微微)**
School of Information and Control Engineering, China University of Petroleum, Dongying 257061, China

Abstract A new method for the voidage measurement of gas-oil two-phase flow was proposed. The voidage measurement was implemented by the identification of flow pattern and a flow pattern specific voidage measurement model. The flow pattern identification was achieved by combining the fuzzy pattern recognition technique and the crude cross-sectional image reconstructed by the simple back projection algorithm. The genetic algorithm and the partial least square method were applied to develop the voidage measurement models. Experimental results show that the proposed method is effective. It can overcome the influence of flow pattern on the voidage measurement, and also has the advantages of simplicity and speediness.
Keywords voidage, two-phase flow, genetic algorithm, tomography, partial least square method

1 INTRODUCTION

Gas-oil two-phase flow exists broadly in chemical, petroleum and metallurgical industries. The voidage is one of the most important parameters of gas-oil two-phase flow. Although many measurement methods are proposed, it is yet difficult to measure the voidage because of the complexity of the two-phase flow. It is necessary to explore new voidage measurement methods[1—3].

The conventional 2-electrode capacitance measurement method has the advantages of simplicity and speediness. Unfortunately, this method is flow pattern dependent. The change of flow pattern may cause great voidage measurement error.

Electrical Capacitance Tomography (ECT), which provides an effective way to reduce the influence of flow pattern on the voidage measurement, is a new technique to measure the voidage and has been studied in recent years. Research work has proved that this technique is an attractive and promising method for the voidage measurement of gas-oil two-phase flow. In conventional voidage measurement methods based on ECT, the voidage values are estimated by the cross-sectional images of the voidage distribution of two-phase flow. A high quality image is necessary to precisely determine the voidage. While reconstructing a high quality image needs a complex and time-consuming image reconstruction algorithm, therefore it is difficult to meet the real-time requirement of the on-line measurement[4—9].

The aim of this work is to propose a new method for the on-line voidage measurement. By this method, the voidage value is estimated by a relevant voidage measurement model, which is a linear optimal capacitance combination based on the genetic algorithm (GA) and the partial least square (PLS) methods. For each flow pattern, a specific voidage measurement model is developed. For the practical voidage measurement, the relevant voidage measurement model is selected according to the real-time but rapid identification result of flow pattern. Thus, the influence of flow pattern on the voidage measurement can be overcome. The identification result of flow pattern is determined by ECT technique and fuzzy pattern recognition technique. Because the crude cross-sectional voidage distribution image is suitable for the use of flow pattern identification, the simple and fast back projection (BP) algorithm is adopted to reconstruct the images. Then, the fuzzy pattern recognition is introduced to complete the identification process. Experimental results show that the proposed voidage measurement method is effective. The proposed method can overcome the influence of flow pattern on the voidage measurement and also has the advantage of speediness.

2 MEASUREMENT SYSTEM

Gas and oil have different dielectric constants (permittivity). The change of the voidage of two-phase flow and its distribution will result in the variation of the measurement capacitances. Using a multi-electrode (*e.g.*, 12 electrodes) capacitance sensor, many capacitance measurements can be obtained pseudo-simultaneously.

Figure 1 shows the schematic structure of the measurement system, which mainly includes a 12-electrode capacitance sensor, a data acquisition unit and a computer.

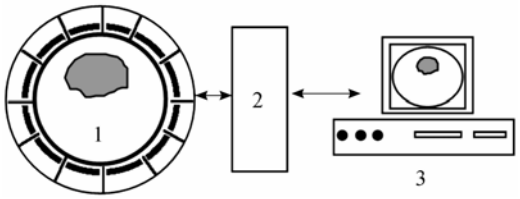

Figure 1 Measurement system
1—sensor; 2—data acquisition unit; 3—computer

The 12-electrode capacitance sensor is shown in Fig.2. It consists of 12 electrodes symmetrically mounted outside an insulating pipe, the projected guard electrodes, the screen, and the insulating pipeline. The measurement system measures the capacitance between all possible combination pairs of the 12 electrodes, converts it into a digital signal, and sends

Received 2006-05-31, accepted 2006-10-16.
* Supported by the National Natural Science Foundation of China (Nos.50576084 and 60532020).
** To whom correspondence should be addressed. E-mail: wangww@hdpu.edu.cn

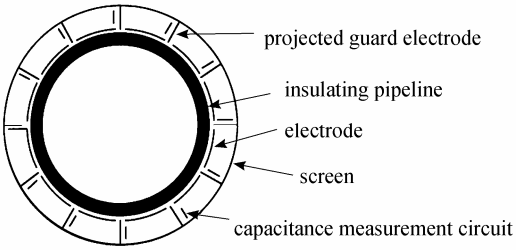

Figure 2 12-electrode capacitance sensor

the data to the computer. The inner diameter of the insulating plexiglass pipe is 50mm and the thickness of this pipe is 4mm. The length of the electrodes is optimized in advance to be 80mm and its width is 20mm. Because of electromagnetic shield the disturbance from outside the sensor have no influence on the measurement[4,10].

The capacitance-to-voltage (C/V) conversion circuit (the capacitance measurement circuit) in the capacitance data acquisition system has the advantages of high data capturing speed, wide dynamic range, stray-immunity, and low base-line drift[10—12]. The C/V circuit boards are fixed on the projected guard electrodes and are connected by a flat cable. Such kind of arrangement can reduce the stray-capacitance, so that the output of the capacitance measurement circuit is less sensitive to the movement of cables outside the sensor. Each electrode is connected to a capacitance measuring circuit (C/V) module. There are 12 modules for a 12-electrode ECT system. The module receives the channel control signal, and then converts the corresponding capacitance measurement to a voltage signal. By subtracting the standard capacitance value (when the pipe is filled with gas) given by a digital-to-analog converter (DAC) from this voltage signal, the capacitance change can be obtained. The resultant capacitance change signal is further amplified by a programmable gain amplifier (PGA) and then digitized by an analog-to-digital converter (ADC). Channel selection, output of the ADC and gain setting of the PGA are carried out by a microcontroller. The results of analog-to-digital conversion are sent to the computer by the micro-controller *via* the serial communication module.

The 12-electrode capacitance sensor can obtain 66 independent capacitance measurements which provide the information of the cross-sectional voidage distribution. According to these capacitances, it is possible to develop a voidage measurement model and estimate the voidage directly. This voidage measurement model should be simple and easy to be implemented. Assuming the voidage of the gas-oil two-phase flow can be calculated by a linear combination of the capacitance measurements, the development of voidage calculation model is converted to a problem of exploring the optimal combination of the measured capacitances. This is a combinatorial optimization problem.

GA is considered as a good algorithm to solve the combinatorial optimization problem. Using GA, it is possible to differentiate the effective capacitances from the ineffective capacitances (the effective capacitance is the one which has significant contribution to the measurement voidage). The weight of the contribution of each effective capacitance is to be determined by the PLS method of regression. Then, the voidage measurement model (the linear relationship between the voidage measurement value and the effective measurement capacitance) is finally developed and will be described in Section 4.

Obviously, it is very difficult to believe that one voidage calculation model could be suitable for the voidage measurements of all different flow patterns. To solve this problem, our scheme is to develop one model for each flow pattern. Meanwhile, the on-line identification result is obtained by using fuzzy pattern recognition technique and the crude cross-sectional images of gas-oil two-phase flow reconstructed by the simple and fast back projection algorithm (will be discussed in Section 3). Thus, the influence of flow pattern on voidage measurement can be overcome.

The flowchart of the whole voidage measurement process is shown in Fig.3. Firstly, the crude cross-sectional gas-oil voidage distribution image is obtained using the simple BP algorithm. Secondly, the flow pattern is identified by combining the fuzzy pattern recognition technique with the obtained crude image. Lastly, according to the identification result of flow pattern, the relevant voidage measurement model is selected to calculate the voidage value.

3 FLOW PATTERN IDENTIFICATION

Flow pattern of two-phase flow is a three-dimensional phenomenon. There are many kinds of flow patterns such as bubbly flow, stratified flow, slug flow and annular flow as shown in Fig.4(a). Voidage is the area fraction of the cross section occupied by the gas phase and is determined by the two-dimensional distribution of two-phase flow in the cross section. At the moment of the voidage measurement, according to the geometrical distribution of the two-phase flow, all the above flow patterns can be generally classified into three typical

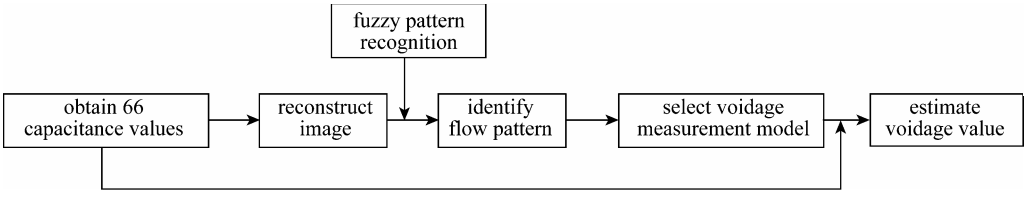

Figure 3 On-line voidage measurement process

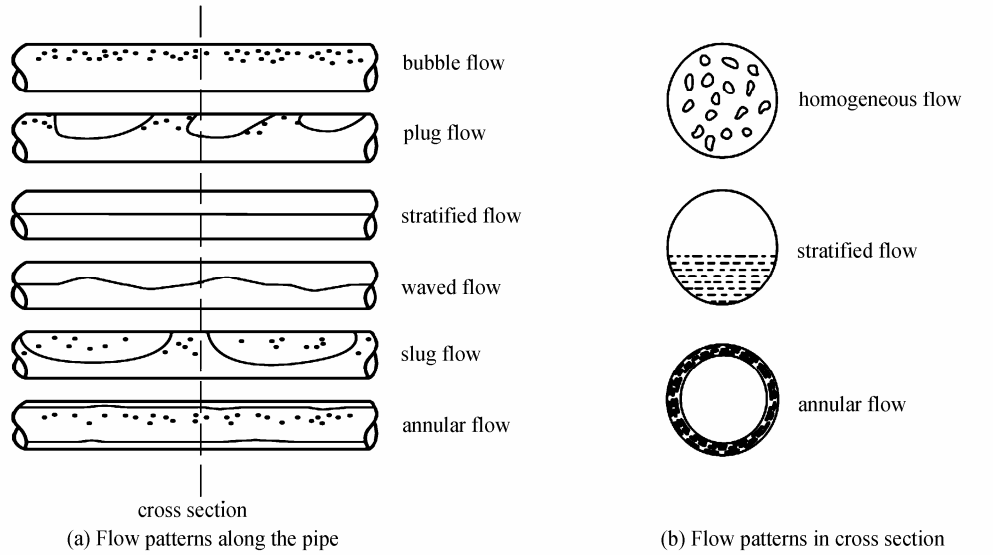

Figure 4 Flow patterns of gas-oil two-phase flow in a horizontal pipe

flow patterns (homogeneous flow, stratified flow and annular flow) as shown in Fig.4(b). For example, bubbly flow can be considered as homogeneous flow, the standard stratified flow and the wavy stratified flow can be treated as stratified flow, and slug flow can be regarded as the combination of stratified flow and homogeneous flow. So, for the measurement of voidage, the aim of flow pattern identification is to identify the real-time flow pattern with either homogeneous, stratified, or annular flow.

The flow pattern identification process can be mainly divided into two steps. Firstly, the crude cross-sectional image, the grey level distribution of gas-oil two-phase flow, is reconstructed using the simple and fast BP algorithm. Secondly, the flow pattern is identified by the fuzzy pattern recognition technique[13].

The whole image area, the cross-sectional area of the pipeline of gas-oil two-phase flow, is divided into 54 pixels (shown in Fig.5). The grey level of each pixel is determined by the simple BP algorithm as following

$$f_j = \sum_{i=1}^{N} c_i s_{ij} \Big/ \sum_{i=1}^{N} s_{ij} \tag{1}$$

where f_j is the grey level of the jth pixel, c_i is the ith normalized capacitance value, s_{ij} is the weight of the jth pixel related to the ith capacitance and s_{ij} is determined by the finite element method[4,5,14].

Flow pattern identification problem can be regarded as a multifactor fuzzy pattern recognition problem. Considering the geometrical characteristics of the three different flow patterns, the fuzzy pattern identification parameters can be determined as follows: (1) x_1, the average grey level of the whole image area, (2) x_2, the absolute value of the difference between the average grey level of the 27 pixels located at the upper half of the image and that of the 27 pixels located at the lower half, (3) x_3, the absolute value of the difference between the average grey level of the 30 pixels around the periphery of the image and that of the 24 pixels located at the center area.

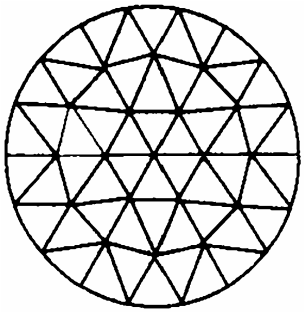

Figure 5 Pixel distribution

Let x_1, x_2 and x_3 denote the fuzzy pattern identification eigenvalues, A_1 (homogeneous flow), A_2 (stratified flow) and A_3 (annular flow) denote the standard patterns, and the normal Gauss distribution function is selected as the membership function. The flow pattern can be obtained according to the maximal membership principle. The membership function set of three standard patterns is given by

$$A_i:\ \mu_i = \left[\mathrm{e}^{-\left(\frac{x_1-\beta_{i1}}{\sigma_{i1}}\right)^2}, \mathrm{e}^{-\left(\frac{x_2-\beta_{i2}}{\sigma_{i2}}\right)^2}, \mathrm{e}^{-\left(\frac{x_3-\beta_{i3}}{\sigma_{i3}}\right)^2} \right] \quad i=1,2,3 \tag{2}$$

where the parameters β_{ij}, σ_{ij} are coefficients determined empirically through a series of experiments. The membership function of the unidentified pattern related to the three standard patterns is given by

$$\mu_{A_i} = \frac{1}{3}\left[\mathrm{e}^{-\left(\frac{x_1-\beta_{i1}}{\sigma_{i1}}\right)^2} + \mathrm{e}^{-\left(\frac{x_2-\beta_{i2}}{\sigma_{i2}}\right)^2} + \mathrm{e}^{-\left(\frac{x_3-\beta_{i3}}{\sigma_{i3}}\right)^2} \right] \quad i=1,2,3 \tag{3}$$

Then, based on the maximal membership principle, the flow pattern is identified. Here β_{ij} and σ_{ij} are determined by experiments, and the typical values of β_{ij} and σ_{ij} are shown as follows:

$$\beta=\begin{bmatrix}1.59 & 0 & 0\\ 0 & 0.96 & 0\\ 0 & 0 & 0.95\end{bmatrix},\quad \sigma=\begin{bmatrix}0.48 & 0.08 & 0.08\\ 0.08 & 1.00 & 0.08\\ 0.08 & 0.08 & 1.00\end{bmatrix} \tag{4}$$

4 VOIDAGE MEASUREMENT MODEL

As mentioned in Section 2, GA and PLS are used to develop the voidage calculation model. To improve the convergence performance, an improved genetic algorithm (IGA) is proposed in this work. The proposed IGA overcomes the disadvantages of time-consuming and local optimization related with the basic GA, and is adopted to obtain the optimal capacitance combination corresponding to each specific flow pattern[15—17]. The modeling process of voidage calculation model is sketched in Fig.6.

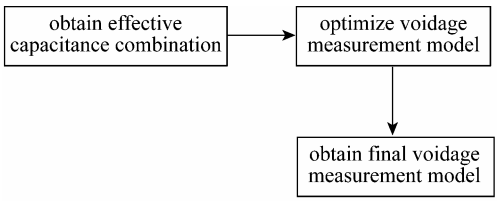

Figure 6 Modeling process of voidage calculation model

4.1 Obtaining the effective capacitance combination using genetic algorithm

The original voidage measurement model is

$$\tilde{\alpha}=\boldsymbol{w}\boldsymbol{c} \tag{5}$$

where $\boldsymbol{c}=[c_1\ c_2\ \cdots\ c_{66}]^{\mathrm{T}}$ is the normalized measurement capacitance vector. $\boldsymbol{w}=[w_1\ w_2\ \cdots\ w_{66}]$ is the coefficient vector, w_i is stochastic initialized at the beginning of the modeling and the value of w_i is 1 or 0 (1 indicates the effective capacitance, and 0 indicates the ineffective capacitance.), $\tilde{\alpha}$ is the estimated voidage. Let α present the actual voidage, to explore the optimal capacitance combination is described as a constrained optimization problem:

$$\begin{aligned}\min_{\boldsymbol{w}\in W} g(w)&=\min_{\boldsymbol{w}\in W}\left|S_\alpha(\alpha)\alpha-\tilde{\alpha}\right|\\ &=\min_{\boldsymbol{w}\in W}\left|S_\alpha(\alpha)\alpha-wc\right|\\ \text{s.t.}\quad & w_i\in\{0,1\}\quad i=1,2,\cdots,66\end{aligned} \tag{6}$$

where $g(w)$ is the objective function, W is the set of the coefficient vectors, $S_\alpha(\alpha)=\tan[(\alpha-a)/b]$ is the nonlinear scale transfer function of the voidage, a and b are determined by experimental data.

The above constrained optimization problem can be solved by using GA[13,15,16]. Two problems exist in the basic genetic algorithm: (1) the opportunity of an individual to be preserved into the next generation is decided by the probability in the proportion of the fitness of this individual; (2) the crossover operator and the mutation operator are pre-determined constants. These two problems cause time-consuming and local optimization of the basic GA. Thus, an improved genetic algorithm (IGA) is proposed in this work.

The nonlinear transform of the fitness function introduced in IGA is to overcome the disadvantage of the local optimization involved in the basic GA. The nonlinear transform of the fitness function is chosen as following

$$\mathrm{fit}_i=\mathrm{e}^{-\gamma f_i} \tag{7}$$

where f_i is the original fitness, fit_i is the transformed fitness, and γ is an adjustable parameter. At the early stage of the algorithm, γ is adjusted to be a larger value to maintain the variety of the population. At the later stage of the algorithm, γ is adjusted to be a smaller value to accelerate the convergence of the algorithm.

Also, on the basis of the elitist strategy, for the further improvement of the convergence speed, the reproduction rate, the crossover rate and the mutation rate of the IGA are reconstructed and change from generation to generation. At the early stage in the algorithm, a relative smaller reproduction rate and a relative larger mutation rate are recommended to improve the average performance of the population. At the later stage in the algorithm, a relative larger reproduction rate and a relative smaller mutation rate are recommended to guarantee the convergence of the algorithm.

The detailed computation procedure of IGA is shown in Fig.7.

4.2 Optimizing the voidage measurement model

PLS method is introduced to optimize the voidage calculation model. PLS method can eliminate the collinearity of the variables and preserve the variance of the variable matrix. The orthogonal components obtained from the variables preserve the essential correlation of the dependent variable with the independent ones, hence, these orthogonal components can be used to develop the final model[18—20].

Using the PLS method, the final voidage measurement model is

$$\tilde{\alpha}=\boldsymbol{w}_f\boldsymbol{c} \tag{8}$$

where $\boldsymbol{w}_f=[w_{f_1}\ w_{f_2}\cdots w_{f_i}\cdots w_{f_{66}}]$ is the regression vector, and the value of w_{fi} is between 0 and 1. The regression vector $\boldsymbol{w}_f$ reflects not only which measurement capacitance is contributive to the voidage measurement but also the quantitative contribution of each effective capacitance.

5 ON-LINE VOIDAGE MEASUREMENT

The flowchart of on-line voidage measurement is shown in Fig.8. Firstly, 66 capacitance values from the ECT sensor are acquired. Secondly, the crude cross-sectional image is reconstructed using the simple BP algorithm and the flow pattern is identified. Lastly, a relevant suitable model corresponding to the

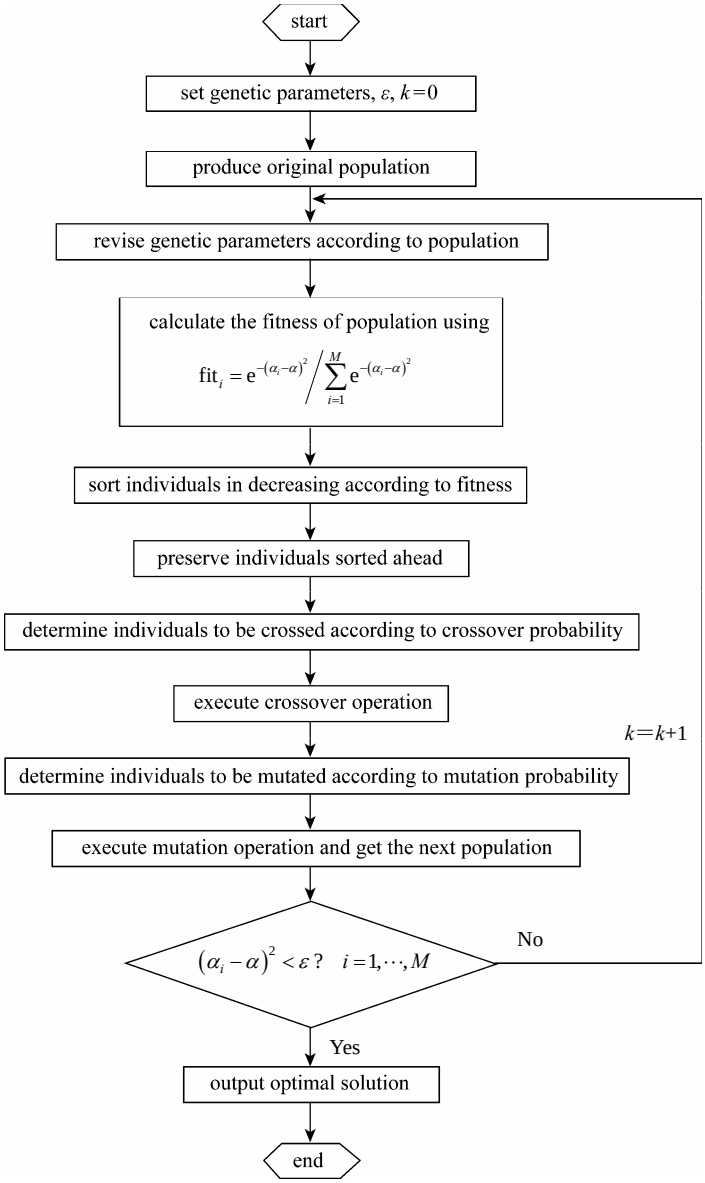

Figure 7 Procedure of IGA

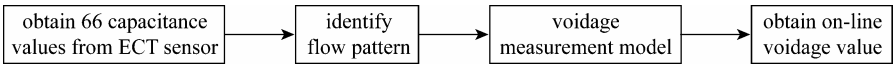

Figure 8 Flowchart of on-line voidage measurement

identified flow pattern is selected to calculate the voidage value.

Because the voidage measurement model is pre-developed and the cross-sectional image is reconstructed by the simple and fast BP algorithm, the voidage measurement can be easily implemented without the complicated and time-consuming computation. That guarantees the real-time performance of voidage measurement.

6 EXPERIMENTAL RESULTS

Because there was no effective dynamic measurement method to obtain the reference voidage data, the static experiments were adopted to verify the proposed voidage measurement method. The experimental materials included gas, diesel oil and thick wall plexiglass tubes (with different inner diameters to simulate bubbles). As mentioned in Section 3, the simulated flow patterns included homogeneous flow, stratified flow and annular flow. The test section was placed horizontally, and the diesel oil was partially filled to simulate the stratified flow. The plexiglass tubes with different inner diameters (simulating bubbles) were placed into the sensor zone, and then the diesel oil was filled into the test section to simulate the homogeneous flow. A small ID plexiglass pipe was placed into the sensor, and the diesel oil was injected

into the gap between the sensor and the plexiglass pipe to simulate the annular flow.

Experimental results were shown in Fig.9. The agreement between the experimental and measured voidage data shows that the voidage measurement was flow pattern independent and the maximum error of the voidage measurement was less than 5%. Meanwhile, the tests showed that the total voidage measurement time was less than 0.1s. The experimental results proved that the accuracy and the real-time performance of the voidage measurement system were satisfactory.

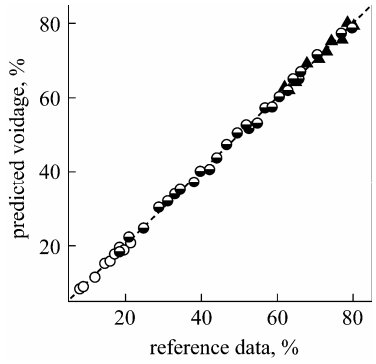

Figure 9 Experimental results
○ homogeneous flow; ◒ stratified flow; ▲ annular flow

7 CONCLUSIONS

Based on ECT technique, GA, and PLS method, a new voidage measurement method is proposed. Experimental results show that the proposed method is effective and flow pattern independent. The maximum error of the voidage measurement is less than 5%, and the total voidage measurement time is less than 0.1 s. The accuracy and the real-time performance of the voidage measurement are satisfactory.

Comparing with the ECT method, the proposed method avoids the complicated and time-consuming image reconstruction process and ensures the real-time performance of the voidage measurement. Comparing with the conventional 2-electrode voidage measurement method, flow pattern identification is introduced in the proposed method and thus the proposed method overcomes the influence of flow pattern on the voidage measurement.

REFERENCES

1 Li, H.Q., Two-Phase Flow Parameter Measurement and Applications, Zhejiang University Press, Hangzhou (1991). (in Chinese)
2 Hewitt, G.F., Measurement of Two Phase Flow Parameters, Academic Press, London (1978).
3 Lin, Z.H., Characteristics of Gas-Liquid Two-phase Flow in Pipelines and Their Engineering Applications, Xi'an Jiaotong University Press, Xi'an (1992). (in Chinese)
4 Li, H.Q., Huang, Z.Y., Special Measurement Technology and Its Applications, Zhejiang University Press, Hangzhou (2000). (in Chinese)
5 Xie, C.G., Huang, S.M., Hoyle, B.S., Thorn, R., Lenn, C., Snowden, D., Beck, M.S., "Electrical capacitance tomography for flow imaging: System model for development of image reconstruction algorithms and design of primary sensors", *IEE Proc. G*, **139**(1), 89—98(1992).
6 Yang ,W.Q., Chondronasios, A., Nattrass, S., Nguyen, V.T., Betting, M., "Adaptive calibration of a capacitance tomography system for imaging water droplet distribution", *Flow Meas. Instrum.*, **15**, 249—258(2004).
7 Yang, W.Q., Liu, S., "Role of tomography in gas/solids flow measurement", *Flow Meas. Instrum.*, **11**, 237—244(2000).
8 Huang, Z.Y., Wang, B.L., Li, H.Q., "Application of electrical capacitance tomography to the void fraction measurement of two-phase flow", *IEEE Trans. Instrum. Meas.*, **52**, 7—12(2003).
9 Huang, Z.Y., Wang, B.L., Li, H.Q., "Dynamic voidage measurements in a gas solid fluidized bed by electrical capacitance tomography", *Chem. Eng. Comm.*, **190**, 1395—1410(2003).
10 Wang, B.L., Ji, H.F., Huang, Z.Y., Li, H.Q., "A high-speed data acquisition system for ECT based on the differential sampling method", *IEEE Sensors J.*, **5**(2), 308—311(2005).
11 Huang, S.M., Xie, C.G., "Design of sensor electronics for electrical cpacitance tomography", *IEE Proc. G*, **139**, 83—88(1992).
12 Yang, W.Q., Stott, A.L., "A high frequency and high resolution capacitance measuring circuit for process tomography", *IEE Proc. Circuits Device Sys.*, **141**, 215—219(1994).
13 Xie, D.L., Huang, Z.Y., Ji, H.F., Li, H.Q., "An online flow pattern identification system for gas-oil two-phase flow using electrical capacitance tomography", *IEEE Trans. Instrum. Meas.*, **55**(5), 1833—1838(2006).
14 Yu, J.H., Ji, H.F., Huang, Z.Y., Li, H.Q., "Skills of finite element method analysis for electrical resistance tomography", *Chinese Journal of Scientific Instrument*, **24**(s4), 687—689(2003). (in Chinese)
15 Xuan, G.N., Cheng, R.W., Genetic Algorithms and Engineering Optimization, Tsinghua University Press, Beijing (2004). (in Chinese)
16 Leite, J.P.B., Topping, B.H.V., "Improved genetic operators for structural engineering optimization", *Adv. Eng. Software*, **29**, 529—562(1998).
17 Han, S.L., Wu, X.J., Ni, M., "Limitation and improved model of GA in combinatorial optimization", *Control Decis.*, **17,** 219—222(2002). (in Chinese)
18 Luinge, H.J., van der Maas, J.H., Visser, T., "Partial least squares regression as a multivariate tool for the interpretation of infrared spectra", *Chemomet. Intel. Lab. Syst.*, **28**, 129—138(1995).
19 Philippe, B., Vincenzo, E.V., Michel, T., "PLS generalised linear regression", *Comput. Stat. Data Anal.*, **48**, 17—46(2005).
20 Preda, C., Saporta, G., "PLS regression on a stochastic process", *Comput. Stat. Data Anal.*, **48**, 149—158(2005).